Turkish Journal of Electrical Engineering & Computer Sciences

http://journals.tubitak.gov.tr/elektrik/

Research Article

Turk J Elec Eng & Comp Sci
(2018) 26: 489 – 500

doi:10.3906/elk-1606-404

RLGC(f) modeling of a busbar distribution system via measured S-parameters at CENELEC and FCC bands

Zeynep HASIRCI*, İsmail Hakkı ÇAVDAR, Mehmet ÖZTÜRK
Department of Electrical & Electronics Engineering, Faculty of Engineering, Karadeniz Technical University, Trabzon, Turkey

Received: 24.06.2016 • **Accepted/Published Online:** 28.06.2017 • **Final Version:** 26.01.2018

Abstract: This paper addresses the extraction of accurate frequency-dependent per-unit-length RLGC parameters for busbar distribution systems using measured S-parameters for the CENELEC and FCC bands. A busbar is a distribution system element (three phase, low voltage) with a modular structure that carries electrical energy in buildings. The S-parameters of a busbar distribution system at different current levels (630 A, 1250 A, 2000 A) are measured with a vector network analyzer and then analyzed for three different two-port connections (L1-N, L2-N, L3-N). A frequency-dependent RLGC(f) model is used to characterize the busbar as a transmission line using a derivative-free optimization algorithm. A time-domain causality check is also conducted. Estimated RLGC parameters are presented along with characteristic impedance and propagation constant. Good agreement has been achieved between measured and estimated S-parameters.

Key words: Busbar distribution system, characteristic impedance, modeling, narrow band, parameter optimization, power line communication, propagation constant, RLGC parameter estimation, smart grid, S-parameters

1. Introduction

Alternative energy sources and increased energy production alone may not be sufficient to ensure a production–consumption balance. Effective and efficient use of energy with control of energy distribution via smart grid applications is also vital. Power line communication (PLC) is a powerful communication alternative that uses the existing grid infrastructure as a communications medium [1–7]. However, a low-voltage (LV) network is more complex than a medium/high-voltage grid due to the need for multipoint communication. A busbar is a modular low-voltage electrical distribution system used within buildings. Such systems are typically found in industrial areas with high power consumption. As issues such as monitoring energy from the point of production to consumption, loss-efficiency analysis, and mobile to mobile communication (M2M) are significant to industry, busbars should be examined in terms of smart grids.

PLC studies on cables have not yielded a complete and accurate identification of busbars. The subject of this study has emerged due to a lack of adequate scientific work. It is necessary to know the characteristics of the busbars for providing PLC communication. Accurate transmission line models are required for the accurate simulation of signal paths implemented in communication systems. Such transmission line models are typically given in per-unit-length parameters (RLGC parameters) to derive the echo transfer function of a power line [8]. While lossy transmission line models may equally be described in terms of characteristic impedance (Z_c)

*Correspondence: zhasirci@ktu.edu.tr

and propagation constant (γ), designers generally focus on RLGC parameters. Busbar systems may also be described as transmission lines [9,10] and represented with RLGC parameters as the other power cables. Many studies have examined the derivation of per-unit-length parameters for power cables. Most of these studies are based on S-parameter measurements [8,11–15], while the remainder are based on time-domain measurements [16–18]. Some methods calculate RLGC parameters from Z_c and γ [8,15,19]. Other methods estimate Z_c from γ extracted from measurements with certain assumptions. Additionally, line parameter extraction is performed using optimization algorithms, including genetic algorithms [20–22].

A few studies about busbars for PLC [9] have examined the S-parameters of a copper conductor series 1000 A busbar system using an EM analysis simulation tool for CENELEC, FCC, and broadband. Hasirci et al. [10] presented the propagation characteristics of different current levels in copper conductor series busbar systems at 1–50 MHz. Some works [9,10] are simulation-based studies that require experimental validation. Because of its widespread use, aluminum type conductor series busbar systems (630 A) have been modeled by Sonnet Suites 13.52. The results were validated with measured S-parameters [23]. Hasirci et al. [24] presented a parameter extraction approach for the 630 A busbar.

In this study, S-parameters of aluminum busbar distribution systems (630 A, 1250 A, 2000 A) were measured with a vector network analyzer (VNA) for the CENELEC and FCC bands. S-parameters are used for Z_c and γ extraction utilizing a casual RLGC(f) model in an optimization process. Additionally, the series impedance components (R, L) and parallel admittance components (C, G) of busbars are presented. The results are examined with error analysis. Good agreement between measured and estimated S-parameters was reached.

2. S-parameter-based characterization

2.1. Technical properties of the busbar

The E-Line KX series busbar distribution system produced by EAE Company [25] is used in this study. Busbars are classified as bolt-on, plug-in, or feeder according to their use and current ratings. They have aluminum or copper conductors. The dielectrics between the conductors are generally polyester or polypropylene. All types of busbar have the same unit length at about 3 m, including connectors.

In this study, busbars of varying currents (630 A, 1250 A, 2000 A) with aluminum conductors were examined. Common technical characteristics are shown in Table 1.

Table 1. Common technical characteristics of E-line KX busbar system (aluminum conductor) [25].

	Abbr.	Unit	Value
Rated current	In	A	630, 1250, 2000
Standards	IEC 61439-6 TS EN 61439-6 IEC 61439-1 TS EN 61439-1		
Rated frequency	f	Hz 50	Protection degree | IP 55
Short-circuit (1 s/peak)	Icw/Ip	kA	25, 60, 80/52.5, 132, 176

Different current levels affect the physical characteristics of the busbar systems. The characteristics of the E-line KX Busbar System for various current levels at 20 °C are listed in Table 2. More detailed information may be found in [25].

Table 2. Physical characteristics of E-line KX busbar system for different current levels at 50 Hz (aluminum conductor) [25].

Current levels, A	Resistance R1, mΩ/m	Reactance X1, mΩ/m	Impedance Z, mΩ/m	Weight, kg/m	Conductor size, mm × mm
630	0.121	0.027	0.124	7.9	6 × 40
1250	0.044	0.013	0.046	13.9	6 × 110
2000	0.026	0.008	0.027	21.7	6 × 200

2.2. General S-parameter representation

As mentioned, a busbar can also be described as a transmission line [9,10] and may be represented with Z_c and γ as with other power cables to determine the transfer function of the communication channel. It is a three-phase system and neutral, and it is analyzed as three different two-port networks, namely L1-N, L2-N, and L3-N. A two-port device is described by parameters including impedance, admittance, and hybrid and voltage/current transmission matrices. For these types of measurements, ideal short/open circuit terminations are required. However, the frequency dependence of such terminations may lead to measurement issues. Thus, S-parameters are a good alternative, overcoming certain measurement faults. S-parameters are defined in terms of traveling waves, unlike terminal voltages and currents, and can be measured on a device located at some distance from the instrument [26]. These measurements are carried out by terminating a port with system impedance Z_o (generally 50 Ω), as shown in Figure 1.

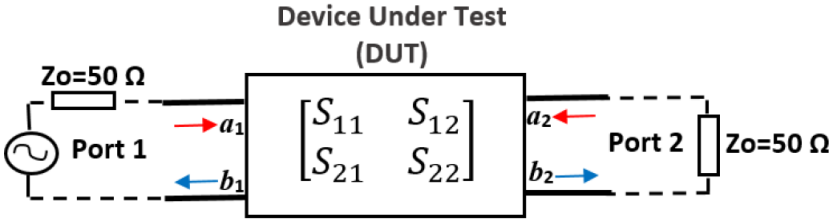

Figure 1. Two-port network with normalized incident waves (a_1, a_2) and reflected waves (b_1, b_2) used in S-parameters.

S-parameters represent the relationship between normalized incident (a_1, a_2) and reflected (b_1, b_2) voltage waves, as shown in Eq. (1).

$$\begin{bmatrix} b_1 \\ b_2 \end{bmatrix} = \begin{bmatrix} S_{11} & S_{12} \\ S_{21} & S_{22} \end{bmatrix} \begin{bmatrix} a_1 \\ a_2 \end{bmatrix} \tag{1}$$

Transmission lines are represented by the infinitesimal length (Δx) element of a transmission line, as illustrated in Figure 2. The telegrapher's equations for transmission lines are as given in Eqs. (2) and (3).

$$\frac{\partial v(x,t)}{\partial x} + Ri(x,t) + L\frac{\partial i(x,t)}{\partial t} = 0 \tag{2}$$

$$\frac{\partial i(x,t)}{\partial x} + Gi(x,t) + C\frac{\partial v(x,t)}{\partial t} = 0 \tag{3}$$

Necessary parameters to determine the transfer function of a transmission line (Z_c and γ) may be calculated

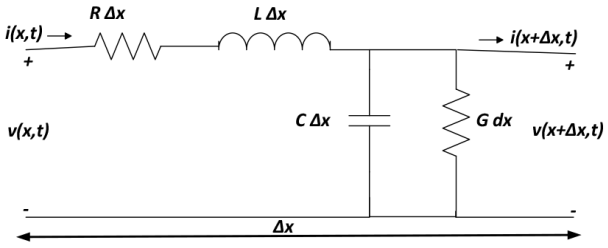

Figure 2. Elementary representation of a transmission line.

as per Eqs. (4) and (5) if per-unit-length parameters are known.

$$Z_c = \sqrt{\frac{R + j\omega L}{G + j\omega C}} \tag{4}$$

$$\gamma = \sqrt{(R + j\omega L)(G + j\omega C)} \tag{5}$$

2.3. Measurement setup

S-parameter measurements were made using a VNA (Agilent Technologies N9913A Field Fox RF Analyzer). The measurement setup is shown in Figure 3. Two 1.5 m length M17/75-RG214 type coaxial cables with 50 Ω characteristic impedance were attached to the ports for the connection between the VNA and the busbars to measure the S-parameters. Two port calibration was used to eliminate unwanted connection effects caused by coaxial cables. These experimental studies were carried out without an extra load connection to determine the transmission line parameters.

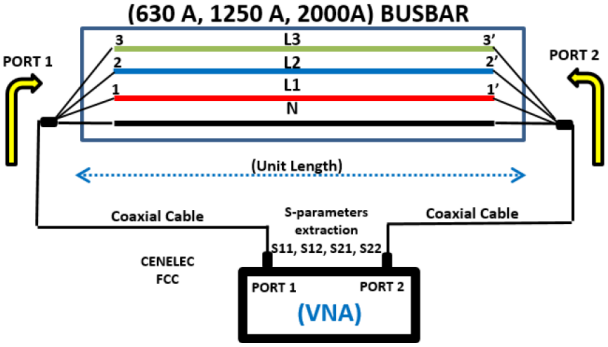

Figure 3. Measurement setup for S-parameters.

3. Application of RLGC(f) model parameter optimization

3.1. Modeling and parameter optimization

There are some conventional and modified transmission line characterization methods that employ VNA measurements [27–30]. This paper uses a frequency-dependent RLGC(f) modeling approach for distributed parameter extraction from measured S-parameters. The results are more accurate and efficient in a broad frequency range because they eliminate discontinuities caused by hyperbolic functions [20–22]. Additionally, the limitations of the conventional methods such as specific line lengths, frequencies, and the number of lines, among others, will be ameliorated.

A derivative-free method was applied to the model parameter optimization process [31]. It aims to find the minimum of a multivariable function based on a simplex search algorithm. This algorithm uses a simplex of $n+1$ points for an n-dimensional parameter vector. It then updates the simplex in five steps: sort, reflection, expansion, outside/inside contraction, and shrink [31]. If the relative change in the objective function value is less than 10^{-4} for 20 successive iterations, the algorithm stops. The error between measured data and the data from the model is calculated with the help of the objective function. The objective function is composed of real and imaginary components of all S-parameters as given in Eq. (6), instead of utilizing only the magnitude of S_{21}. Experiments were conducted using only the magnitudes of S_{21} with relatively significant estimation errors, especially on S_{11}. Thus, by including real and imaginary parts of all S-parameters in the objective function, the optimized unit length elements of transmission line parameters allow the more accurate measurement of data.

$$F_{obj} = \sum_{i=1}^{N} \left| S_{j1}^{measured}(f_i) - S_{j1}^{estimated}(f_i) \right|^2 \quad j \in [1, 2] \tag{6}$$

The transmission line model used for busbars is a simple and common RLGC(f) model [22] as given in Eq. (7). R_1, R_2, G_1, and G_2 refer to DC resistance, skin effect loss, shunt current due to free electrons in an imperfect dielectric (DC conductance), and power loss due to dielectric polarization, respectively.

$$\begin{aligned} R\ (\Omega\ /\ m) &\approx R_1 + R_2\sqrt{f} \quad L\ (H\ /\ m) \approx cons. \\ G\ (S\ /\ m) &\approx G_1 + G_2 f \quad C\ (F\ /\ m) \approx cons. \end{aligned} \tag{7}$$

As with all optimization algorithms, the selection of initial parameters is as important as the definition of the objective function. The closeness of the initial values is set at the global minimum to maximize the convergence rate of the algorithm. The search range for each parameter is inspired from that of a parallel plate transmission line due to the similarities with the signal paths of a busbar [22]. After that, a trial and error procedure is applied on parameter search bounds to make better estimation intervals. Finally, bounds providing a minimum objective function value are selected. The overall parameter estimation process is given as a flowchart in Figure 4.

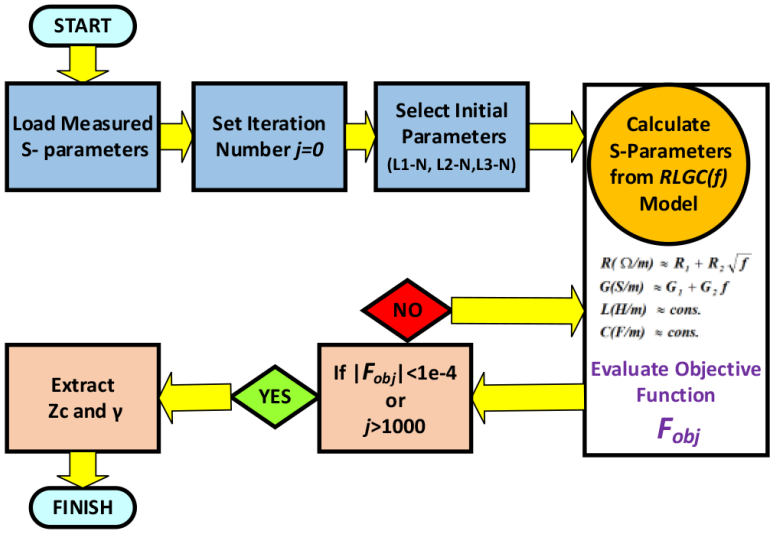

Figure 4. Optimization process flowchart of the model parameter extraction.

3.2. Error analysis

Comparisons of measured and estimated S-parameters for different port connections (L1-N, L2-N, L3-N) of 630 A, 1250 A, and 2000 A current level busbars are given as amplitude and phase graphs in Figures 5–7, respectively. The results show good agreement. Due to the objective function's use of measured S-parameters, visual presentations of results are given as a qualitative analysis. Secondly, in quantitative analysis, error statistics between measured and estimated S-parameters are listed in Tables 3–5 for 630 A, 1250 A, and 2000 A current level busbars, respectively.

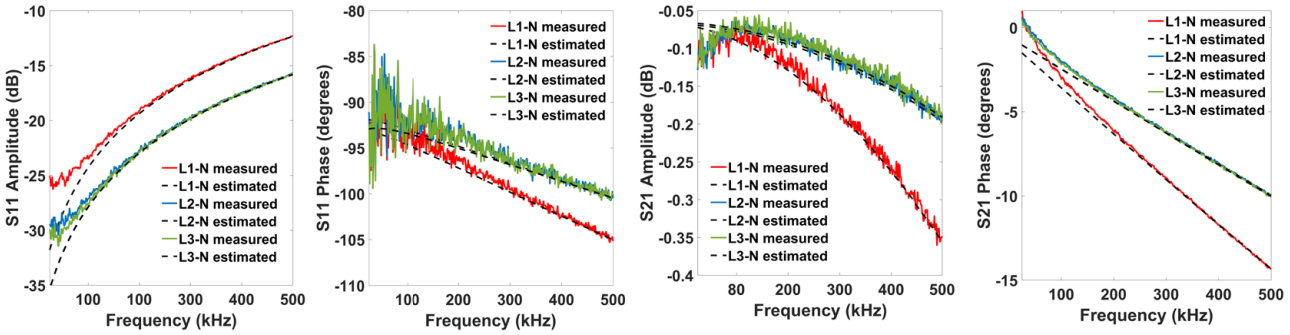

Figure 5. Measured and estimated S_{11} and S_{21} parameters for 630 A aluminum busbar.

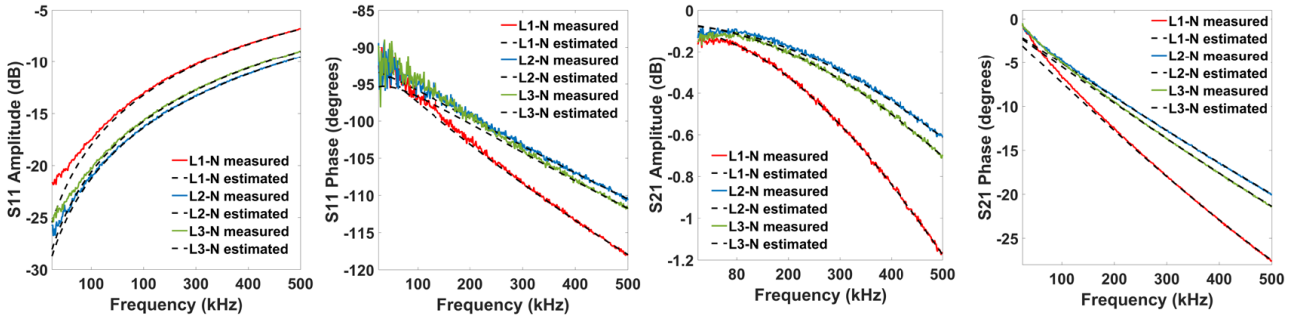

Figure 6. Measured and estimated S_{11} and S_{21} parameters for 1250 A aluminum busbar.

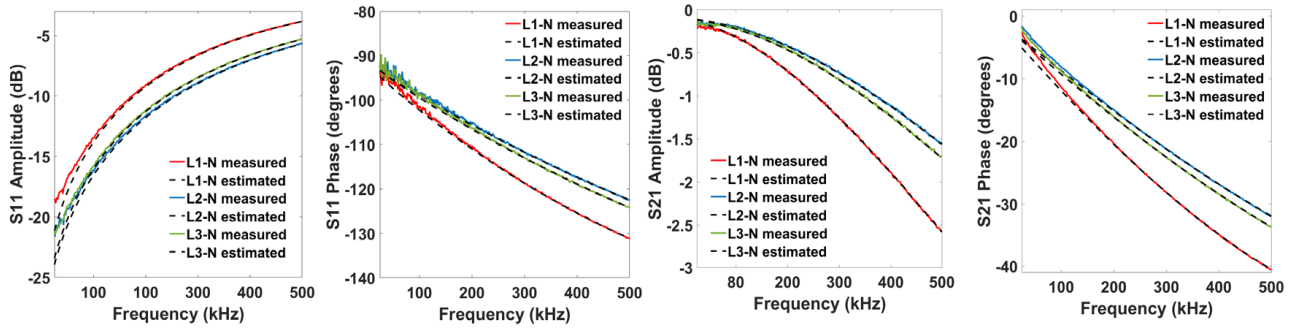

Figure 7. Measured and Estimated S11 and S21 parameters for 2000 A aluminum busbar.

Error analysis is carried out on the cumulative distribution function (CDF) of estimation error. Since the error distribution is not homogeneous along the frequency axis, the error calculated in the objective function, which is the mean error, would not reflect the actual performance due to the sensitivity of mean error to outliers.

Table 3. Estimation error with 90% possibility for 630 A aluminum busbar.

	S11 (dB)	S11 (°)	S21 (dB)	S21 (°)
L1-N	$\leq 0.910 - 0.970$	$\leq 0.859 - 1.260$	$\leq 0.017 - 0.018$	$\leq 0.572 - 0.630$
L2-N	$\leq 0.751 - 0.819$	$\leq 1.867 - 2.051$	$\leq 0.015 - 0.016$	$\leq 0.475 - 0.487$
L3-N	$\leq 0.380 - 0.456$	$\leq 1.776 - 1.948$	$\leq 0.016 - 0.017$	$\leq 0.356 - 0.372$

Table 4. Estimation error with 90% possibility for 1250 A aluminum busbar.

	S11 (dB)	S11 (°)	S21 (dB)	S21 (°)
L1-N	$\leq 0.530 - 0.570$	$\leq 0.742 - 0.866$	$\leq 0.690 - 0.713$	$\leq 0.572 - 0.630$
L2-N	$\leq 0.165 - 0.198$	$\leq 0.763 - 0.953$	$\leq 0.321 - 0.336$	$\leq 0.475 - 0.487$
L3-N	$\leq 0.310 - 0.349$	$\leq 1.822 - 1.990$	$\leq 0.018 - 0.019$	$\leq 0.475 - 0.492$

Table 5. Estimation error with 90% possibility for 2000 A aluminum busbar.

	S11 (dB)	S11 (°)	S21 (dB)	S21 (°)
L1-N	$\leq 0.331 - 0.364$	$\leq 0.619 - 0.708$	$\leq 0.033 - 0.034$	$\leq 0.598 - 0.621$
L2-N	$\leq 0.380 - 0.418$	$\leq 0.604 - 0.704$	$\leq 0.020 - 0.021$	$\leq 0.561 - 0.578$
L3-N	$\leq 0.232 - 0.261$	$\leq 0.392 - 0.522$	$\leq 0.019 - 0.021$	$\leq 0.435 - 0.453$

Instead, the CDF is used to show the mean error for 90% of the data. In this way, a mean estimation error with 90% possibility is presented.

The data dealt with here are discrete, which means that distribution functions will be defined in some small width of data range known as a bin. The two numbers given in each cell of all tables represent the bounds of the corresponding bin.

4. Results

If parallel admittance components (G, C) and series impedance components (R, L) are known for a given transmission line, γ and Z_c can be calculated. These parameters are estimated with the help of Eq. (7) for three different port connections for each busbar type. Obtained results are given in Figure 8 for 630 A, 1250 A, and 2000 A current level busbars, respectively. Additionally, estimated R, L, G, and C values are presented as shown in Figures 9–11 for each busbar type. Z_c and γ can be calculated via Eqs. (4) and (5) using estimated per-unit-length parameters.

A causality check is necessary to demonstrate the performance of the model in representing the physical system. There are two methods: time-domain and frequency-domain. In this study, the time-domain method is selected based on checking received signals. A pulse signal is sent, and the received signal is observed. When a certain start point can be seen in the received signal, which occurs after the input pulse, the model used is causal. An example of a time-domain causality check for only the L1-N port connection of the 630 A current level busbar is shown in Figure 12. Attenuation can also be evidently seen in the same figure. When the same check is replicated for all port connections of studied busbars, the results show that the model is causal for all conditions.

5. Discussion

It is essential to know the characteristics of busbar distribution systems for providing PLC communication. In this study, busbar distribution systems (630 A, 1250 A, 2000 A) were modeled as a transmission line with measured S-parameters at the CENELEC and FCC bands. Increasing frequency reveals skin effect and

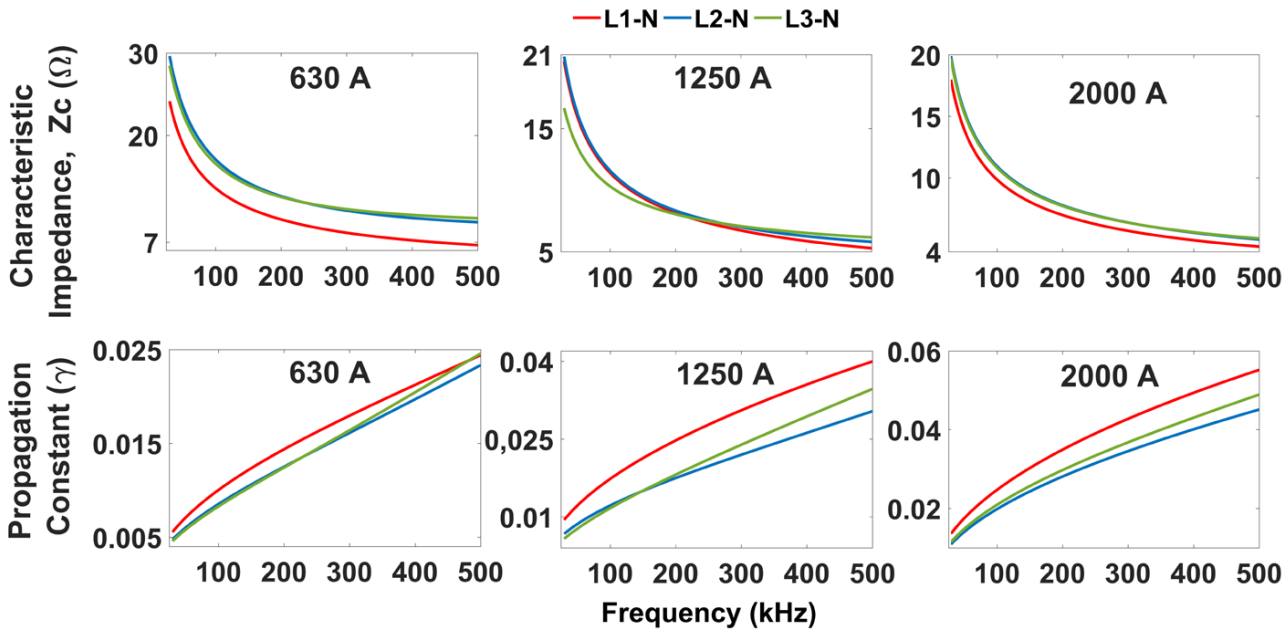

Figure 8. Extracted Zc and γ for L1-N, L2-N, and L3-N port connections for 630 A, 1250 A, and 2000 A aluminum busbars.

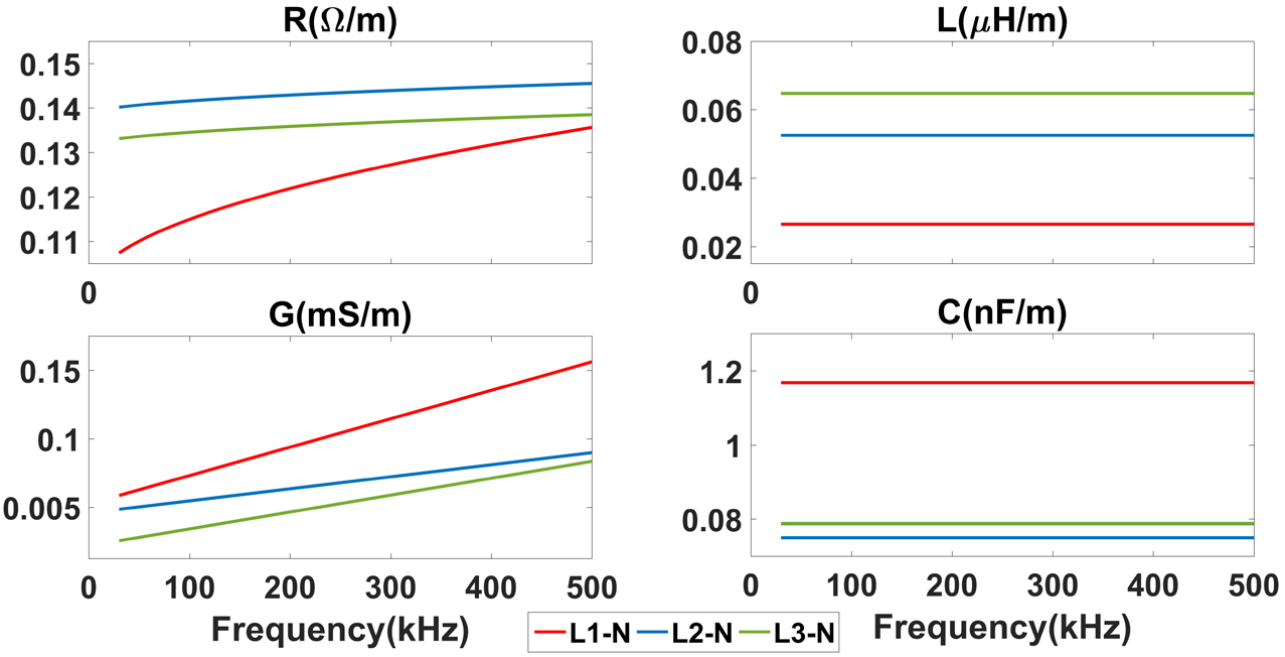

Figure 9. Estimated RLGC parameters of 630 A busbar from measured S-parameters for three different port connections.

dispersion, which cause the frequency dependence on per-unit-length parameters of the busbar distribution system. Therefore, a frequency-dependent RLGC(f) model was used for busbar modeling. Model parameters were estimated with a simplex-based derivative-free optimization algorithm. The error between measured and estimated S-parameters was analyzed (Tables 3–5). The quantitative results show that estimated S-parameters

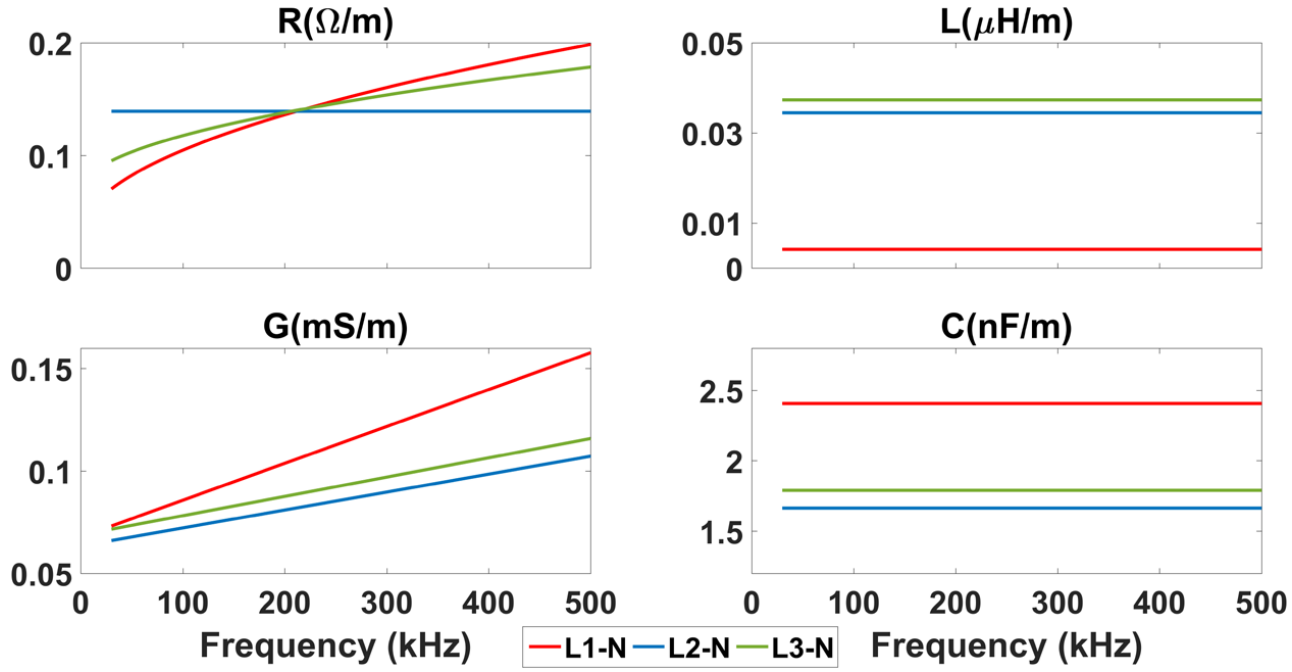

Figure 10. Estimated RLGC parameters of 1250 A busbar from measured S-parameters for three different port connections.

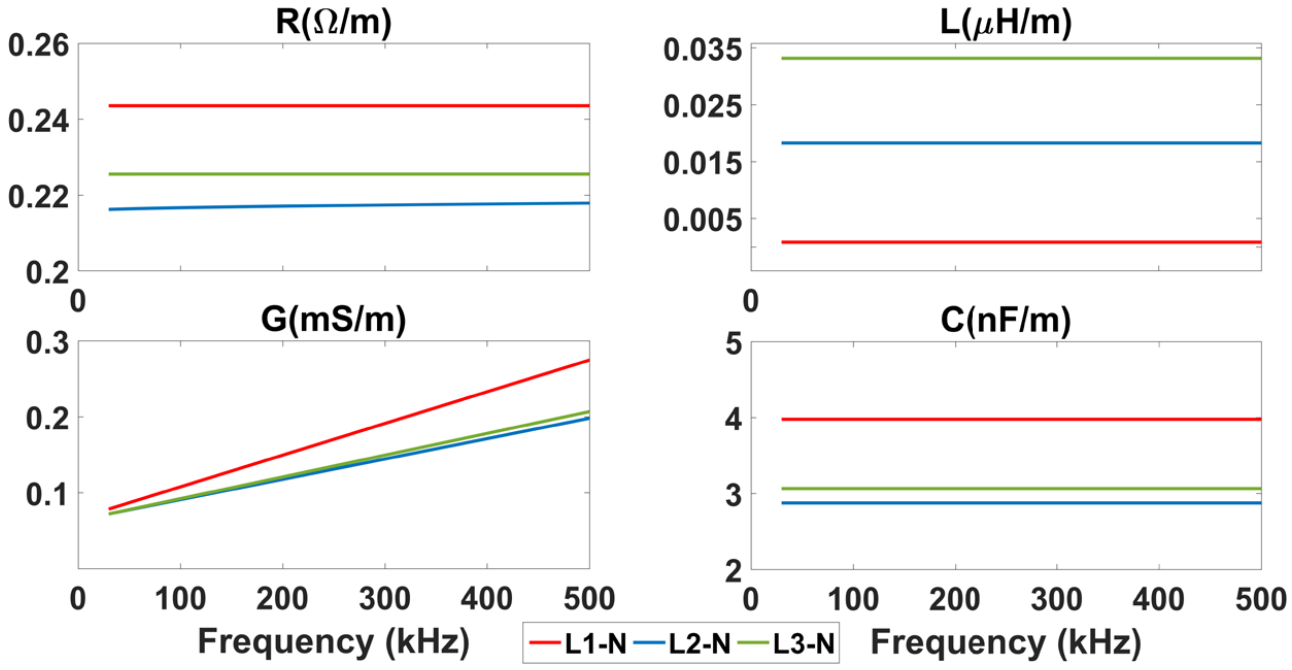

Figure 11. Estimated RLGC parameters of 2000 A busbar from measured S-parameters for three different port connections.

coincide with the measured ones. The maximum mean estimation error values for magnitudes S_{11} and S_{21} are 0.97 dB, and 0.7 dB, respectively. Additionally, the maximum values of mean phase errors are smaller than 2° and 0.63° for S_{11} and S_{21}, respectively. Good frequency-domain correlation between measurement

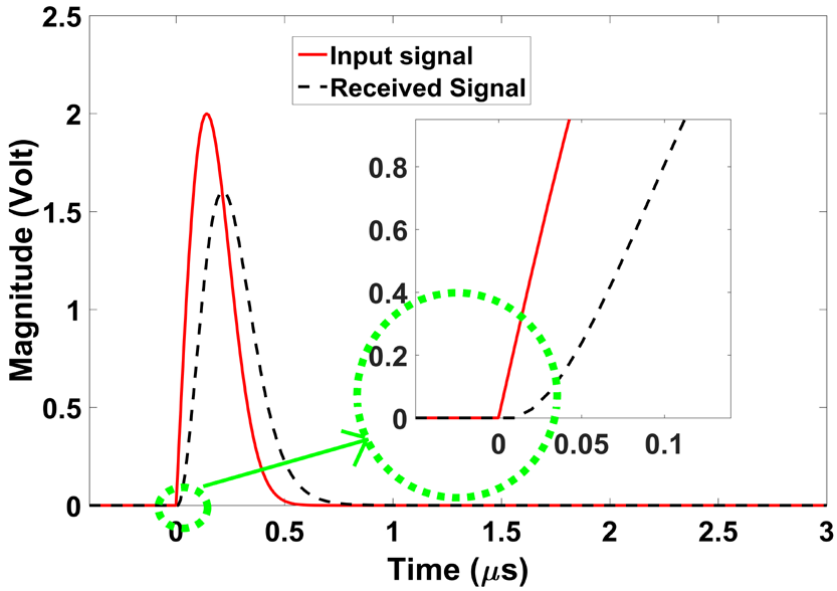

Figure 12. An example of causality check for L1-N port connection for 630 A aluminum busbar.

and modeling approach has been achieved. Additionally, a time-domain causality check was conducted for all conditions to determine the causality of the RLGC(f) model (Figure 12).

The results obtained for RLGC values show that distributed inductance decreases with an increase in cross-section area. Distributed capacitance is increased as expected for the same reason (Figures 9–11). Z_c and γ were extracted from estimated RLGC values (Figure 8). Z_c values typically decrease with frequency, unlike γ, which increases. Moreover, Z_c values are smaller for the L1-N port connection for all types of busbars, while γ shows higher values for the same configuration.

The transmission line theory determines the transfer function of the PLC channel using a bottom-up approach. Towards this aim, network topology must be defined in terms of the properties of the network components, including cables, lines, loads, and so on. To summarize, the results of this study are vital in determining the characteristics of the busbar distribution systems to provide PLC communication at the CENELEC and FCC bands. The outcomes demonstrate that for modeling other types of busbars in this frequency range, this type of modeling approach can be used. For higher frequency applications such as broadband PLC, improved RLGC(f) modeling may be needed due to greater frequency dispersion of the dielectric material.

Acknowledgments

This work was supported by the TÜBİTAK (the Scientific and Technological Research Council of Turkey), 1003 - Primary Subjects R&D Funding Program, Project No: EEEAG-115E137. The authors would also like to thank EAE Company for their support in providing the busbar distribution systems.

References

[1] Schwartz M. History of Communications - Carrier-wave telephony over power lines: early history. IEEE Commun Mag 2009; 47: 14-18.

[2] Dostert K. Power Line Communications. Upper Saddle River, NJ, USA: Prentice Hall, 2001.

[3] Ferreira H, Lampe L, Newbury J, Swart T. Power Line Communications. 1st ed. New York, NY, USA: John Wiley & Sons, 2010.

[4] Latchman H, Yonge L. Power line local area networking (guest editorial). IEEE Commun Mag 2003; 41: 32-33.

[5] Pavlidou N, Vinck AH, Yazdani J, Honary B. Power line communications: state of the art and future trends. IEEE Commun Mag 2003; 41: 34-40.

[6] Galli S, Scaglione A, Dostert K. Broadband is power: Internet access through the power line network (guest editorial). IEEE Commun Mag 2003; 41: 82-83.

[7] Biglieri E, Galli S, Lee YW, Poor H, Vinck H. Power line communications (guest editorial). IEEE J Sel Areas Commun 2006; 24: 1261-1266.

[8] Papazyan R, Petterson P, Edin H, Eriksson R, Gafvert U. Extraction of High Frequency Power Cable Characteristics from S-parameter Measurements. IEEE T Dielect El In 2004; 11: 461-470.

[9] Hasirci Z, Cavdar IH. Modeling of high power busbar systems for power line communications. In: IEEE International Energy Conference; 13–16 May 2014; Dubrovnik, Croatia. New York, NY, USA: IEEE. pp. 1515-1519.

[10] Hasirci Z, Cavdar IH, Suljanovic N, Mujcic A. Investigation of current variation effect on PLC channel characteristics of LV high power busbar systems. In: 5th IEEE PES Innovative Smart Grid Technologies European Conference; 12–15 October 2014; İstanbul, Turkey. New York, NY, USA: IEEE. pp. 1-5.

[11] Marks RB, Williams DF. Characteristic impedance determination using propagation constant measurement. IEEE Microwave Guided Wave Lett 1991; 1: 141-143.

[12] Goldberg SB, Steer MB, Franzon PD. Experimental electrical characterization of interconnects and discontinuities in high-speed digital systems. IEEE T Compon Hybr 1991; 14: 761-765.

[13] Williams DF, Rogers JE, Holloway CL. Multiconductor transmission-line characterization: representations, approximations, and accuracy. IEEE T Microw Theory 1999; 47: 403-409.

[14] Chen G, Zhu L, Melde K. Extraction of frequency dependent RLCG parameters of the packaging interconnects on low-loss substrates from frequency domain measurements. In: 14th Topical Meeting on Electrical Performance of Electronic Packaging; 24–26 October 2005. New York, NY, USA: IEEE. pp. 25-28.

[15] Kim J, Han D. Hybrid method for frequency-dependent lossy coupled transmission line characterization and modeling. In: Electrical Performance of Electronic Packaging; 27–29 October 2003; Princeton, NJ, USA. New York, NY, USA: IEEE. pp. 239-242.

[16] Deutsch A, Arjavalingam G, Kopcsay GV. Characterization of resistive transmission lines by short-pulse propagation. IEEE Microw Guided W 1992; 2: 25-27.

[17] Ferrari P, Flechet B, Angenieux G. Time domain characterization of lossy arbitrary characteristic impedance transmission lines. IEEE Microw Guided W 1994; 4: 177-179.

[18] Kim W, Lee S, Seo M, Swaminathan M, Tummala R. Determination of propagation constants of transmission lines using 1-port TDR measurements. In: 59th ARFTG Conference Digest; 7 June 2002; Seattle, WA, USA. New York, NY, USA: IEEE. pp. 119-126.

[19] Degerstrom MJ, Gilbert BK, Daniel ES. Accurate resistance, inductance, capacitance, and conductance (RLCG) from uniform transmission line measurements. In: Electrical Performance of Electronic Packaging; 27–29 October 2008; San Jose, CA, USA. New York, NY, USA: IEEE. pp. 77-80.

[20] Zhang J, Chen QB, Qiu Z, Drewniak JL, Orlandi A. Extraction of causal RLGC models from measurements for signal link path analysis. In: 2008 International Symposium on Electromagnetic Compatibility - EMC Europe; 8–12 September 2008; Hamburg, Germany. New York, NY, USA: IEEE. pp. 1-6.

[21] Zhang J, Drewniak JL, Pommerenke DJ, Koledintseva MY, Dubroff RE, Cheng W, Yang Z, Chen QB, Orlandi A. Causal RLGC(f) models for transmission lines from measured S-parameters. IEEE T Electromagn C 2010; 52: 189-198.

[22] Zhang J, Koledintseva MY, Drewniak JL, Antonini G, Orlandi A. Extracting R, L, G, C parameters of dispersive planar transmission lines from measured S-parameters using a genetic algorithm. In: International Symposium on Electromagnetic Compatibility EMC 2004; 9–13 August 2004; Eindhoven, the Netherlands. New York, NY, USA: IEEE. pp. 572-576.

[23] Hasirci Z, Cavdar IH. Extraction of narrowband propagation properties of a 630 A current level busbar. In: 39th International Conference on Telecommunications and Signal Processing; 27–29 June 2016; Vienna, Austria. New York, NY, USA: IEEE. pp. 203-206.

[24] Hasirci Z, Cavdar IH, Ozturk M. Estimation of propagation parameters for aluminum busbar up to 500 kHz. In: 2016 International Symposium on Innovations in Intelligent Systems and Applications; 2–5 August 2016; Sinaia, Romania. New York, NY, USA: IEEE. pp. 1-4.

[25] EAE Company. E-Line KX Busbar Power Distribution System (Datasheet). Ankara, Turkey: EAE Company, 2016.

[26] Gupta KC, Garg R, Chadha R. Computer-Aided Design of Microwave Circuits. New York, NY, USA: Artech House, 1981.

[27] Sampath MK. On addressing the practical issues in the extraction of RLGC parameters for lossy multi-conductor transmission lines using S-parameter models. In: Electrical Performance of Electronic Packaging; 27–29 October 2008; San Jose, CA, USA. New York, NY, USA: IEEE. pp. 259-262.

[28] Marks RB. A multiline method of network analyzer calibration. IEEE T Microw Theory 1991; 39: 1205-1215.

[29] Kim J, Han DH. Hybrid method for frequency-dependent lossy coupled transmission line characterization and modelling. In: 12th Topical Meeting on Electrical Performance of Electronic Packaging; 27–29 October 2003; Princeton, NJ, USA. New York, NY, USA: IEEE. pp. 239-242.

[30] Narita K, Kushta T. An accurate experimental method for characterizing transmission lines embedded in multilayer printed circuit boards. IEEE T Adv Packaging 2006; 29: 114-121.

[31] Lagarias JC, Reeds JA, Wright MH, Wright PE. Convergence properties of the Nelder-Mead simplex method in low dimensions. SIAM J Optimiz 1998; 9: 112-147.